

Graphene-MoS₂ Hybrid Structure Enhanced Fiber Optic Surface Plasmon Resonance Sensor

Wei Wei^{1,2,3} · Jinpeng Nong^{1,2,3} · Linlong Tang³ · Ning Wang^{1,2} · Chin-Jung Chuang^{3,4} · Yu Huang^{1,2,3}

Received: 3 July 2016 / Accepted: 29 August 2016 / Published online: 9 September 2016
© Springer Science+Business Media New York 2016

Abstract In this paper, a fiber optic surface plasmon resonance sensor based on graphene-MoS₂ hybrid structure is presented. The wavelength interrogation method is employed to analyze the reflection spectra and the performance of the sensor. The theoretical analysis shows that the confined electric field generated at the interface between the sensor surface and the surrounding environment can be enhanced by introducing graphene-molybdenum disulfide (MoS₂) hybrid structure as the sensing layers coated on the core of fiber. Such electric field enhancement significantly improves the sensitivity of the fiber optic surface plasmon resonance sensor. Furthermore, it is suggested that coating more number of graphene and MoS₂ layers on thicker Au film is a good selection for the higher enhancement of the sensitivity. The sensitivity of the proposed sensor exhibits an enhancement of 20 % compared to that of the conventional fiber optic surface plasmon resonance sensing scheme without graphene-MoS₂ hybrid structure. The proposed graphene-MoS₂-Au fiber optic surface plasmon resonance sensor is simple in structure, has high sensitivity, and shows good potential in practical applications.

Keywords Sensor · Fiber · Surface plasmon resonance · Graphene · MoS₂

Introduction

Surface plasmon resonance (SPR) has gained a wide attention among physicists, chemists, and biochemists due to its unique properties that can be utilized for a variety of applications including food safety, human health care, and environmental monitoring [1–3]. Surface plasmons are the coherent oscillations of conduction electrons at the interface between the noble metal and the external dielectric. The plasmonic spectral response of SPR to a change in the refractive index of the external environment in contact with the metal film plays a critical role in chemical and biological sensing technology. The most conventional approach to excite surface plasmon is using the Kretschmann configuration, where a prism is coupled with a thin metal film [3]. Whereas the prism-based SPR sensor has a number of shortcomings such as large size and the difficulties of remote sensing. Fortunately, this can be compensated by replacing the prism with an optical fiber. In such a classic structure, light is delivered into the core of optical fiber through total internal reflection, and an evanescent field is generated at the vicinity of metal-dielectric interface where the surface plasmon resonance is induced. Since the surface plasmon wave is lossy, the coupling strength depends dramatically on the refractive index of the external environment around the metal layer. One important advancement of fiber optic SPR sensor is that it is substantially miniaturized and is highly portable for measurements outside the laboratory environment. More importantly, fiber optic SPR sensor exhibits additional advantages such as low-cost component, remote sensing, and multichannel performance for high-throughput screening applications.

✉ Wei Wei
wwei@cqu.edu.cn

✉ Yu Huang
huangyu@cigit.ac.cn

¹ Key Laboratory of Optoelectronic Technology and Systems, Ministry of Education of China, Chongqing University, Chongqing 400044, China

² College of Optoelectronic Engineering, Chongqing University, Chongqing 400044, China

³ Chongqing Institute of Green and Intelligent Technology, Chinese Academy of Sciences, Chongqing 400714, China

⁴ Department of Opto-Electronic Engineering, National Dong Hwa University, Hualien, Taiwan 97401, China

Despite these advantages, the performance of fiber optic SPR sensor still requires some improvements in order to approach the sensitivity of traditional prism-based SPR sensor. Several attempts have been made to improve the sensitivity of fiber optic SPR sensor, such as controlling the chemical interactions at the sensor surface [4, 5], modifying the geometry of sensor probe [6, 7], and implementing signal amplification strategy using Au nanoparticle [8] and nanomaterials [5]. Although many materials have been introduced to enhance the sensitivity of the fiber optic SPR sensor, graphene is a one of the most extensively studied two-dimensional nanomaterials due to its unique optical/electrical properties [9–13]. The relatively large surface area of graphene allows it to have a better surface contact with the analyte [10]. Compared to the gold surface, the graphene adsorbs biomolecules more strongly and stably due to the π -stacking interactions between graphene's hexagonal cells and the carbon-based ring structures [11, 14]. SPR sensor based on graphene-on-gold has been investigated to enhance the performance of sensor [15, 16]. However, it was reported that the sensitivity improvement of graphene-based SPR sensors is limited due to the low optical absorption and direct zero band gap of graphene [15, 17].

More recently, ultra-thin layer of molybdenum disulfide (MoS_2) that belongs to the transition-metal dichalcogenide (TMDC) semi-conductor group is recently discovered in the vast of two-dimensional nanomaterials [18–20]. It is regarded as “beyond graphene” nanocrystal material composed of two-dimensional layers stacked in the vertical direction via van der Waals force. When the thickness of MoS_2 crystal is thinned down to monolayer of ~ 0.65 nm, a new electronic and optical property can be generated [10]. The band gap of bulk MoS_2 is indirect of 1.2 eV, whereas the monolayer MoS_2 has a direct band gap of 1.8 eV due to quantum confinement effects [21, 22]. Optical absorption efficiency of monolayer MoS_2 is $\sim 5\%$, which is higher than that of graphene layer of $\sim 2.3\%$. More importantly, the electron energy loss of MoS_2 layer is comparable to that of the graphene layer, which allows a successful ($\sim 100\%$) light energy transfer to the graphene- MoS_2 -coated sensing substrate [10]. Such process will give rise to a significant enhancement of SPR signals.

Loan et al. had demonstrated the sensor with graphene- MoS_2 hybrid nanostructures for selective detection of DNA hybridization [20]. Zeng et al. has investigated the enhanced performance of graphene- MoS_2 hybrid nanostructures prism-based SPR sensor compared to the conventional sensor without graphene- MoS_2 structure or only have graphene [17]. In this study, the hybrid nanostructure of graphene- MoS_2 -Au is introduced as the sensing layers coated on the core of fiber. The electrons are able to be

transferred from Au film to MoS_2 and graphene layers under optical excitation because the work function of Au is higher than that of MoS_2 and graphene [23, 24]. The optical response of fiber optic SPR sensor coated with graphene- MoS_2 hybrid nanostructures has been systematically investigated in term of Au film thickness and number of MoS_2 and graphene layers.

Sensor Layout and Analysis

The structure of the sensing head under analysis is schematically illustrated in Fig. 1. The sensing region is an uncladded fiber core with the diameter of D , coated with a sheet of Au film with the thickness of d_1 , and the MoS_2 sensing layer with the thickness of d_2 ($d_2 = N_1 \times 0.65$ nm [25], where N_1 is the number of MoS_2 layers) and the graphene sensing layer with the thickness of d_3 ($d_3 = N_2 \times 0.34$ nm [25], where N_2 is the number of graphene layers). The sensing layers of MoS_2 and graphene are in contact with the analyte with the refractive index of n_s .

The wavelength-dependent dielectric constant of core in the fiber is given by [26, 27]

$$n_1(\lambda) = \sqrt{1 + \frac{A_1\lambda^2}{\lambda^2 - B_1^2} + \frac{A_2\lambda^2}{\lambda^2 - B_2^2} + \frac{A_3\lambda^2}{\lambda^2 - B_3^2}}, \quad (1)$$

where Sellmeier coefficients $A_1 = 0.6961663$, $A_2 = 0.6961663$, $A_3 = 0.8774794$, $B_1 = 0.4079426$, $B_2 = 0.0684043$, $B_3 = 9.896161$, and λ is the wavelength of incident light.

The relative permittivity of gold in the sensing region is described by Drude-Lorentz model [27]:

$$\epsilon_{DL}(\omega) = \epsilon_\infty - \frac{\omega_D^2}{\omega(\omega + i\gamma_D)} - \frac{\Delta\epsilon\Omega_L^2}{(\omega^2 + \Omega_L^2) + i\Gamma_L\omega}, \quad (2)$$

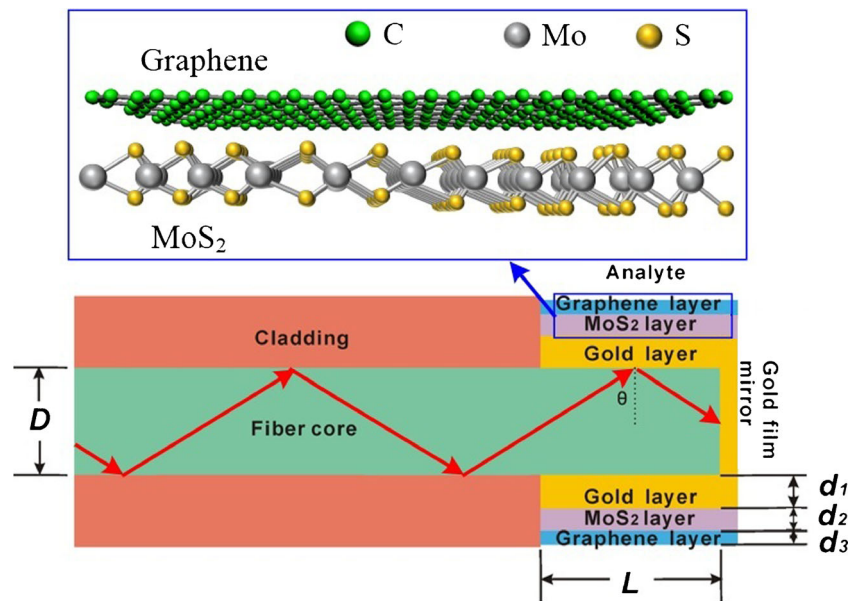
where ω is the angular frequency of light, ϵ_∞ is the dimensionless high frequency limit contributed from interband transition of electrons, ω_D is plasmon frequency, γ_D is the damping coefficient due to the dispersion of the electrons, $\Delta\epsilon$ is a weight factor, and Ω_L and Γ_L are the strength and spectral width of the Lorentz oscillator, respectively.

The complex refractive index of monolayer MoS_2 in the visible region is obtained from the experimental measurement data by Yim [28]. The complex refractive index of monolayer graphene in the visible is given as [29]

$$n_3 = 3.0 + i\frac{C_1}{3}\lambda, \quad (3)$$

where the constant $C_1 \approx 5.446 \mu\text{m}^{-1}$ is implied by the opacity measurement by Nair [30].

Fig. 1 Schematic diagram of the proposed fiber optic SPR sensor with graphene-MoS₂ hybrid structure



The light is launched into one end of the fiber at the axial point and reflected at the other end. The normalized transmitted power of light can be derived as Eq. (4), by using the reflectance value for a single reflection at the core/Au interface

$$P = \frac{\int_{\theta = \theta_{cr}}^{\theta = \pi/2} R_P^{N_{ref}(\theta)} P(\theta) d\theta}{\int_{\theta = \theta_{cr}}^{\theta = \pi/2} P(\theta) d\theta}, \tag{4}$$

where $P(\theta)$ is the angular reflected power distribution transmitted expressed as

$$P(\theta) = \frac{n_1^2 \sin\theta \cos\theta}{(1 - n_1^2 \cos^2\theta)^2}, \tag{5}$$

$R_P = |r_p|^2$ is the reflection intensity, $N_{ref}(\theta) = \frac{2L}{D \tan\theta}$ is the total number of light reflections performed in the fiber optic SPR sensor by a ray whose incident angle is θ with the normal to the core-Au layer interface in the sensing region with the length of L , $\theta_{cr} = 90 - \arcsin\left(\frac{NA}{n_1}\right)$ is the critical angle of the fiber, and NA is its numerical aperture. Because of the long distance between the input end of optical fiber and the sensitive area, the polarization effect of different launched rays is neglected. Based on the proposed fiber optic SPR sensor structure, the parameters used for this study are numerical aperture of fiber NA = 0.22, the length of exposed sensing length $L = 10$ mm, and fiber core diameter $D = 600$ μm .

Results and Discussion

Figure 2a shows the reflection spectra of the sensors for four different structures at the refractive index of 1.333. It is observed that the presence of MoS₂ monolayer or graphene monolayer is able to shift the spectra to longer wavelength region, especially the simultaneous presence of MoS₂ monolayer and graphene monolayer. This is attributed to the large value of the real part of the dielectric function of MoS₂ and graphene layer.

To evaluate the sensing performance of the sensor, the calculated resonant wavelength λ_{res} as a function of the refractive index is plotted in Fig. 2b. One can see that the resonant wavelength experiences a non-linear red shift as the refractive index varies from 1.333 to 1.373. The sensitivity of the sensor can be obtained from the slope of these curves, which is defined as

$$S_n = \frac{\delta\lambda_{res}}{\delta n_s}, \tag{6}$$

where δn_s is the change in refractive index of solution and $\delta\lambda_{res}$ is the corresponding resonant wavelength shift. Their sensitivity in the range from 1.341 to 1.373 is given in Table 1. It can be seen that the sensitivity for the conventional sensor (structure 1) is minimum, whereas the presence of monolayer graphene (structure 2) could improve the sensitivity of the sensor. Compared to the sensitivity enhancement produced by the monolayer graphene, the improvement of sensitivity induced by the presence of monolayer MoS₂ (structure 3) is slightly slower at the small refractive index region. However, its enhancement capability for sensitivity surpassed that by the presence of monolayer graphene at higher refractive index region. The presence of both monolayer MoS₂ and

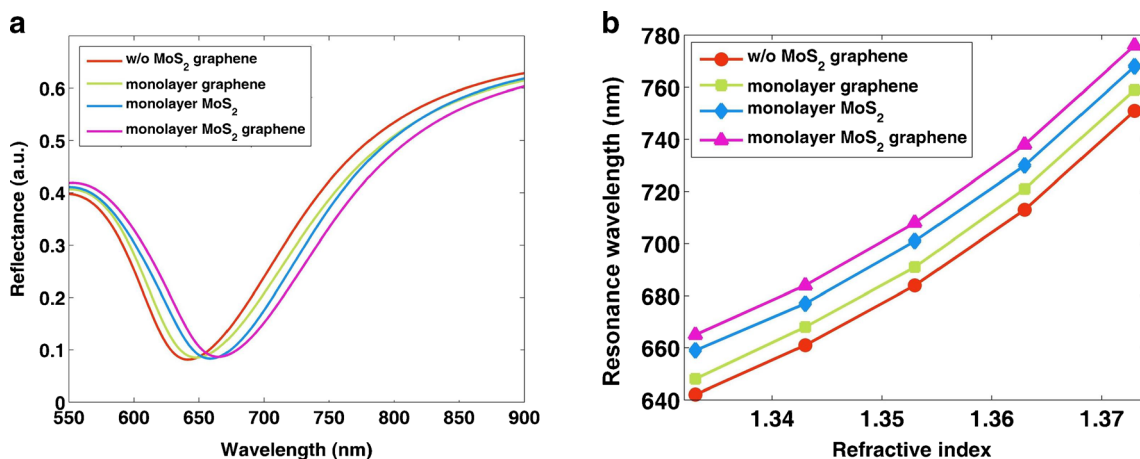


Fig. 2 **a** Reflection spectra of the proposed fiber optic SPR sensor for structure without (w/o) MoS₂-graphene layers, with MoS₂ monolayer, with graphene monolayer, and with MoS₂ monolayer and graphene

monolayer at refractive index of 1.333. **b** The relationship between the resonant wavelength λ_{res} and refractive index. The thickness of the gold layer is 50 nm

monolayer graphene exhibits comprehensive effect on the sensitivity of the sensor (structure 4), which possesses better sensing performance than the structure using only graphene or only MoS₂ layer.

To further explain the sensitivity enhancement mechanism by the present of monolayer MoS₂ and monolayer graphene, finite element analysis method is employed using COMSOL Multiphysics to analyze the electric field distribution surrounding the graphene-MoS₂ hybrid nanostructures, as shown in Fig. 3a. A highly confined electric field is generated at the graphene-MoS₂ monolayer interface with intensity of 6.6×10^4 V/m, which significantly enhances the interaction between the light and the sensing medium. To illustrate the penetration characteristic of the electric field, the electric field intensity along the direction (Au-MoS₂-graphene) perpendicular to sensing interface is further extracted and compared with that of three other structures in Fig. 3b. It is observed that the electric field generated by graphene-MoS₂ monolayer structure is the strongest and exponentially decays into the sensing medium. The penetration depth is defined as the distance where the electric field intensity decreased to be 1/e. For the graphene-MoS₂ monolayer structure, the penetration depth of the electric field into the sensing medium is 205 nm, which is larger than that of three other structures (190 nm for structure 1, 198 nm for structure 2, and 200 nm for structure 3). Thus, the introduction of both MoS₂ and

graphene sensing layers can enhance the intensity of the electric field surrounding the sensing layer and enables the sensor to be more sensitive to the change of medium.

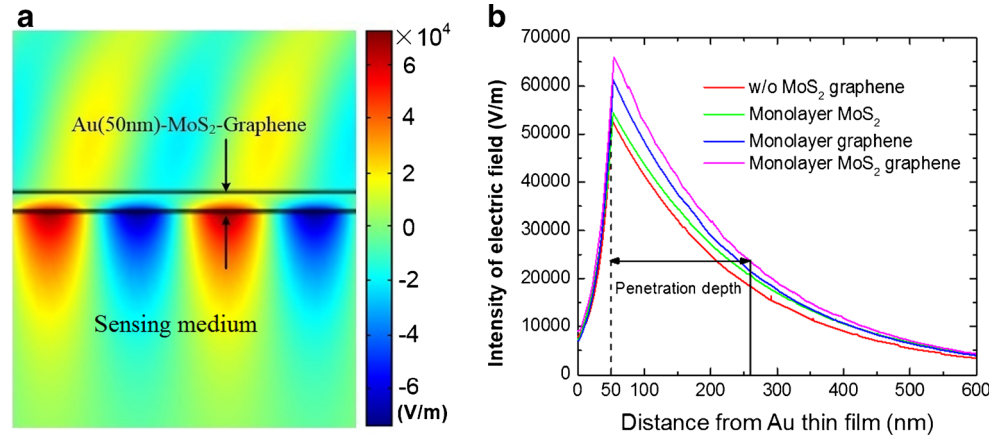
We then investigate the modulation of the number of the MoS₂ and graphene layers on the resonance spectra of the sensor. The effect of the number of the graphene layers on the resonance spectra is first analyzed. Figure 4a presents the reflection spectra with varying number of graphene layers for the structure with monolayer MoS₂ covered on the Au film. One can see that the resonant wavelength red shifts from 658.7 to 692.5 nm as the number of graphene layers increases from zero to five, along with the increase of the minimum reflectance and the bandwidth. The reason is attributed to the fact that graphene is a lossy dielectric having complex dielectric constant [31]. Hence, the damping associated with the surface plasmon wave in the graphene region increases as the number of graphene layers increases, which results in the shallowing and broadening of the reflection curve.

Then, the influence of the number of MoS₂ layers on the resonance spectra is explored. The reflection spectra with varying number of the number of MoS₂ layers for the structure with monolayer graphene covered on Au film are sketched in Fig. 4b. It reveals that the SPR resonant wavelength exhibits a larger red shift (from 646.9 to 721.6 nm) with increasing number of MoS₂ layers compared to that with increasing number of graphene layers. This is because that MoS₂ has a larger real

Table 1 Sensitivity for four different structures for refractive index at 1.341, 1.353, 1.361, and 1.373. The unit of the sensitivity S_n is nm/RIU

Structure no.	Layers in the structure	S_n $n_s = 1.341$	S_n $n_s = 1.353$	S_n $n_s = 1.361$	S_n $n_s = 1.373$
1	Without MoS ₂ and graphene	1977	2731	3234	3800
2	Monolayer graphene, w/o MoS ₂	2043	2780	3272	3825
3	Monolayer MoS ₂ , w/o graphene	1970	2742	3251	3835
4	Monolayer MoS ₂ , monolayer graphene	2037	2791	3294	3860

Fig. 3 **a** Electric field distribution of graphene-MoS₂ hybrid structure at the resonant wavelength of 665 nm. **b** Cross-section plot of the total electric field along the direction perpendicular to the sensing interface



part of dielectric function than graphene, and thereby a longer wavelength is required to excite SPR [10]. However, the minimum reflectance decreases as the number of MoS₂ layers increases, which is contrary to the case with increasing graphene layers. It can be attributed to the fact that the optical absorption of MoS₂ monolayer is higher than that of graphene monolayer. Consequently, the absorption of the structure can be effectively enhanced and thereby promote a stronger SPR excitation [32].

These characteristics of the resonance spectra significantly influence the sensing performance of the fiber optic SPR sensors. The variation of the sensitivity in accordance with the number of MoS₂ and graphene layers when the refractive index of the medium is changed from 1.333 to 1.343 and 1.353 to 1.363 is plotted in Fig. 5a, b, respectively. One can see that the sensitivity increases as the number of graphene and MoS₂ layers increases. For the refractive index range from 1.333 to 1.343 (Fig. 5a), maximum sensitivity of 2290 nm/RIU can be achieved for the sensor with five layers of MoS₂

and six layers of graphene, which improves by 20 % with respect to that of the sensor without MoS₂ and graphene layer. While for the refractive index range from 1.353 to 1.363 (Fig. 5b), maximum sensitivity of 3440 nm/RIU can be obtained for the sensor with four layers of MoS₂ and six layers of graphene, which improves by 18 % with respect to that of the sensor without MoS₂ and graphene layer. This indicates that coating more graphene and MoS₂ layers on the Au film is a favorable option to enhance the sensitivity of the fiber optic SPR sensor.

Meanwhile, an abnormal phenomenon is observed from Fig. 5a that the sensitivity increases with fluctuation as the number of MoS₂ layers increases for the fixed number of graphene layers. This is different from Fig. 5b that the sensitivity increases monotonously. Such phenomenon is ascribed to the fact that the sensitivity of the sensor is inversely proportional to the slope of the real part of the wavelength-dependent dielectric function [33]. Specifically, when the refractive index of the medium is changed from 1.333 to 1.343

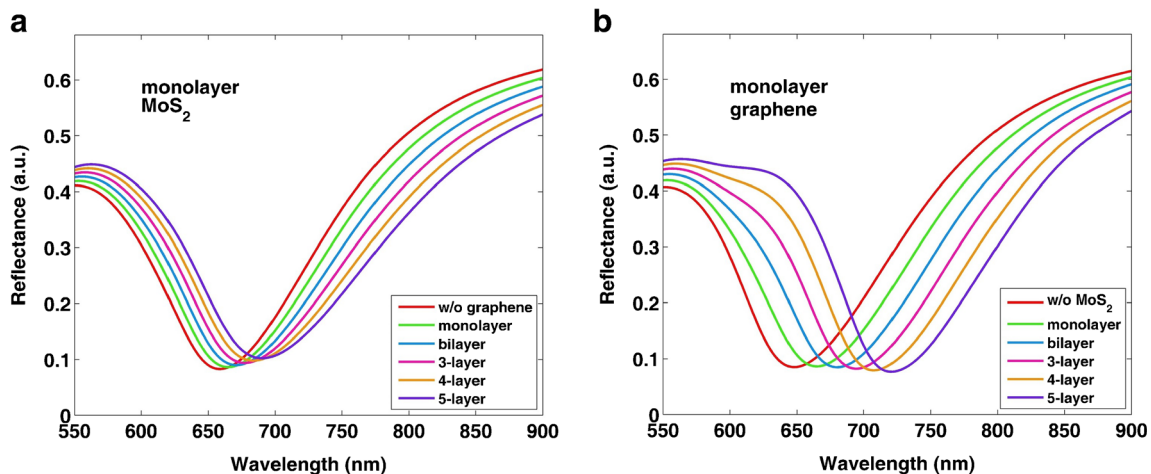


Fig. 4 **a** Variation of reflection spectra in accordance with the number of graphene layers for the structure with monolayer MoS₂. **b** Variation of reflection spectra in accordance with the number of MoS₂ layers for the

structure with monolayer graphene. The thickness of Au film is 50 nm, and the refractive index of the sensing medium is 1.333

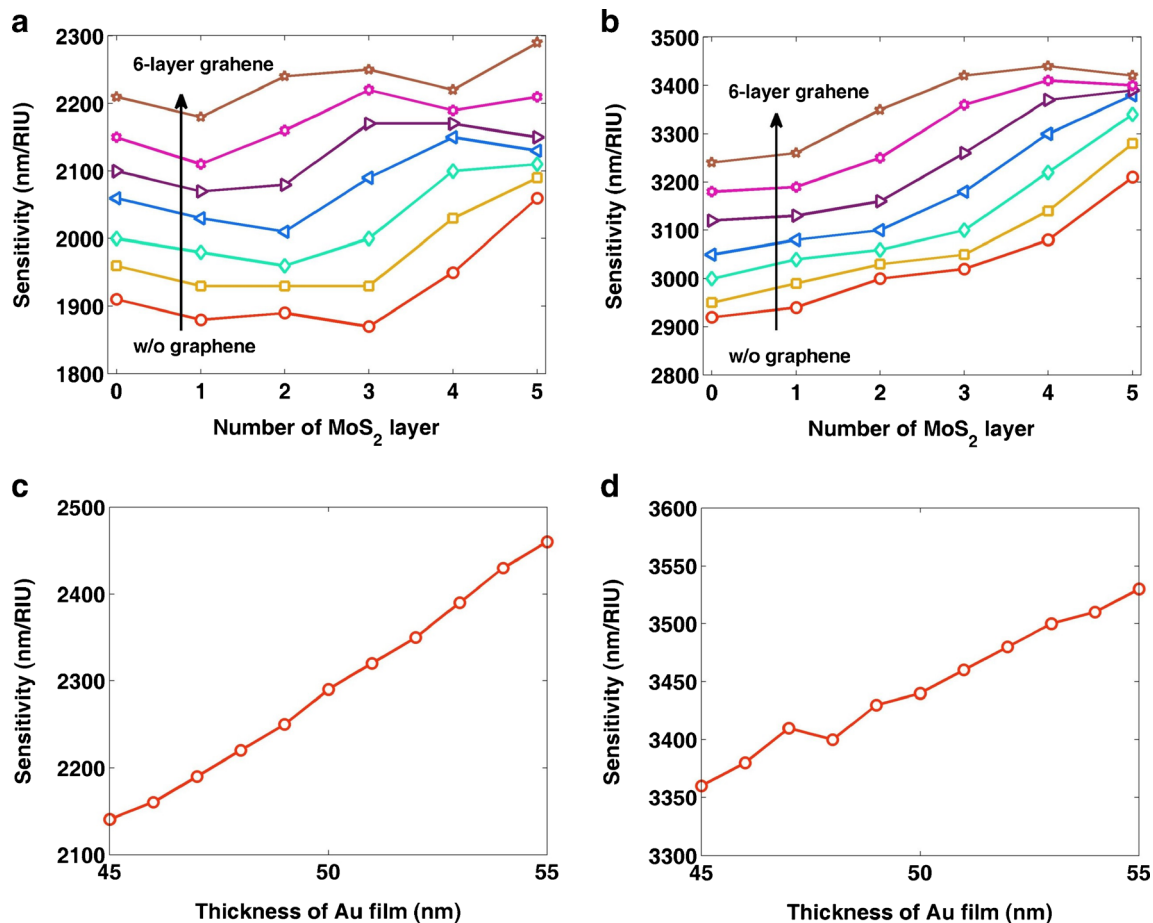


Fig. 5 Variation of the sensitivity in accordance with varying number of MoS₂ and graphene layers. Thickness of the gold layer is 50 nm. The refractive index is changed from 1.333 to 1.343 (a) and 1.353 to 1.363 (b). Change of sensitivity at various thickness of Au film due to the

change of refractive index from 1.333 to 1.343 for the sensor with five layers of MoS₂ and six layers of graphene (c) and from 1.353 to 1.363 for the sensor with four layers of MoS₂ and six layers of graphene (d)

(Fig. 5a), the resonant wavelength of the sensor with varying number of MoS₂ and graphene layers locates in the range of 650 ~ 750 nm (Fig. 4a, b). In this range, the slope of the real part of MoS₂ dielectric function initially increases with increasing resonant wavelength, and then exhibits a reduction with a fluctuation when the wavelength exceeds 700 nm [28]. While the slope of the real part of graphene dielectric function continually decreases [29]. The comprehensive enhancement effect of graphene and MoS₂ results in this nonmonotonic variation tendency. While when the refractive index is between 1.353 and 1.363 (Fig. 5b), the resonant wavelength of the sensor initially presents beyond 700 nm. In this range, both the slopes of the real part of MoS₂ and graphene dielectric function decrease with increasing resonant wavelength as the number of MoS₂ and graphene layer increases. Consequently, the sensitivity exhibits a monotonous variation tendency. In addition, the sensitivity would saturate when the number of MoS₂ and graphene layers is large enough, due to the loss induced by the over-absorption of MoS₂ and graphene against their enhancement effect [10].

Finally, the thickness of Au film is optimized to improve the sensitivity of the sensor. Figure 5c, d illustrate the sensitivity as a function of Au film thickness in the case of fiber optic SPR sensor with optimal configuration perturbed by the change of refractive index from 1.333 to 1.343 and 1.353 to 1.363, respectively. One can obviously see that the sensitivity increases monotonously as the thickness of Au film increases from 45 to 55 nm. It is known that the reflected power occurs when the energy and momentum of the surface plasmon mode and the corresponding fiber mode match to each other. The reflected power around either side of the resonant wavelength depends on the coupling of surface plasmon mode and fiber mode. The coupling of two modes is dependent on the thickness of Au film. Thinner metallic layers produce more interaction between fiber mode and surface plasmon mode. Consequently, more light would be absorbed by the sensing region, resulted in decreased reflected power. This, in turn, causes an increase in the sensitivity with an increase in Au film thickness [34]. In practices, the thickness of Au film, and the number of MoS₂ and graphene layers are adjustable according to the fabrication technique and cost to achieve

desirable sensing performance for the proposed fiber optic SPR sensor.

Conclusion

In this paper, a highly sensitive fiber optic SPR sensor based on graphene-MoS₂ hybrid nanostructure is presented. The resonant wavelength of the proposed sensor experiences red shift with the presence of MoS₂ and graphene layer. The numerical analysis shows that the presence of graphene-MoS₂ hybrid nanostructure significantly enhances the electric field at the interface between nanostructure and adjacent medium. Such graphene-MoS₂ hybrid nanostructure is able to improve the sensitivity of fiber optic SPR sensor compared to the conventional fiber optic SPR sensing scheme without graphene-MoS₂. Hence, it is believed that the proposed sensor shows great potentials in the future biomolecule sensing application.

Acknowledgments This work is supported by the Visiting Scholar Foundation of Key Laboratory of Optoelectronic Technology and Systems (Chongqing University), Ministry of Education, National High Technology Research and Development Program of China (Grant No. 2015AA034801), the National Natural Science Foundation of China (Grant No. 61307103, 61405021), the Action Plan for Western Development of Chinese Academy of Sciences (Grant No. KZCX2-XB3-14), the STS Project of Chinese Academy of Sciences (Grant No. KFJ-EW-ST5-011), the Chinese Academy of Sciences Visiting Program for Taiwan Youth (Grant No. 2015TW2GB0001), the Natural Science Foundation of Chongqing, China (Grant No. cstc2014jcyjA40045), and the Scientific Research Foundation for the Returned Overseas Chinese Scholars, State Education Ministry.

References

1. Srivastava SK, Gupta BD (2011) Influence of ions on the surface plasmon resonance spectrum of a fiber optic refractive index sensor. *Sensors Actuators B Chem* 156(2):559–562. doi:10.1016/j.snb.2011.01.068
2. Wei W, Nong J, Tang L, Zhang G, Jiang X, Zhu Y (2015) Reflection-type infrared biosensor based on surface plasmonics in graphene ribbon arrays. *Chin Opt Lett* 13(8):082801–082805. doi:10.3788/col201513.082801
3. Roh S, Chung T, Lee B (2011) Overview of the characteristics of micro- and nano-structured surface plasmon resonance sensors. *Sensors* 11(2):1565–1588. doi:10.3390/s110201565
4. Arghir I, Delpont F, Spasic D, Lammertyn J (2015) Smart design of fiber optic surfaces for improved plasmonic biosensing. *New Biotechnol* 32(5):473–484. doi:10.1016/j.nbt.2015.03.012
5. Ravi Shankaran D, Miura N (2007) Trends in interfacial design for surface plasmon resonance based immunoassays. *Appl Phys* 40(23):7187–7200. doi:10.1088/0022-3727/40/23/s02
6. Srivastava SK, Gupta BD (2011) A multitapered fiber-optic SPR sensor with enhanced sensitivity. *IEEE Photon Technol Lett* 23(13):923–925. doi:10.1109/LPT.2011.2146767
7. Caucheteur C, Guo T, Albert J (2015) Review of plasmonic fiber optic biochemical sensors: improving the limit of detection. *Anal Bioanal Chem* 407(14):3883–3897. doi:10.1007/s00216-014-8411-6
8. Wang L, Li T, Du Y, Chen C, Li B, Zhou M, Dong S (2010) Au NPs-enhanced surface plasmon resonance for sensitive detection of mercury(II) ions. *Biosensors & Bioelectronics* 25(12):2622–2626. doi:10.1016/j.bios.2010.04.027
9. Novoselov KS, Geim AK, Morozov SV, Jiang D, Zhang Y, Dubonos SV, Grigorieva IV, Firsov AA (2004) Electric field effect in atomically thin carbon films. *Science* 306(5696):666–669. doi:10.1126/science.1102896
10. Zeng S, Hu S, Xia J, Anderson T, Dinh X-Q, Meng X-M, Coquet P, Yong K-T (2015) Graphene-MoS₂ hybrid nanostructures enhanced surface plasmon resonance biosensors. *Sensors Actuators B Chem* 207:801–810. doi:10.1016/j.snb.2014.10.124
11. Maurya JB, Prajapati YK, Singh V, Saini JP (2015) Sensitivity enhancement of surface plasmon resonance sensor based on graphene-MoS₂ hybrid structure with TiO₂-SiO₂ composite layer. *Applied Physics A* 121(2):525–533. doi:10.1007/s00339-015-9442-3
12. Wu J (2016) Tunable ultranarrow spectrum selective absorption in a graphene monolayer at terahertz frequency. *Appl Phys* 49(21):215108. doi:10.1088/0022-3727/49/21/215108
13. Qian H, Ma Y, Yang Q, Chen B, Liu Y, Guo X, Lin S, Ruan J, Liu X, Tong L, Lin Wang Z (2014) Electrical tuning of surface plasmon polariton propagation in graphene-nanowire hybrid structure. *ACS Nano* 8(3):2584–2589. doi:10.1021/nn406221s
14. Wei W, Nong J, Tang L, Zhang G, Yang J, Luo W (2016) Conformal graphene-decorated nanofluidic sensors based on surface plasmons at infrared frequencies. *Sensors* 16(6). doi:10.3390/s16060899
15. Wu L, Chu HS, Koh WS, Li EP (2010) Highly sensitive graphene biosensors based on surface plasmon resonance. *Opt Express* 18(14):14395–14400. doi:10.1364/OE.18.014395
16. Verma A, Prakash A, Tripathi R (2014) Performance analysis of graphene based surface plasmon resonance biosensors for detection of pseudomonas-like bacteria. *Opt Quant Electron* 47(5):1197–1205. doi:10.1007/s11082-014-9976-1
17. Choi SH, Kim YL, Byun KM (2011) Graphene-on-silver substrates for sensitive surface plasmon resonance imaging biosensors. *Opt Express* 19(2):458–466. doi:10.1364/OE.19.000458
18. Du J, Wang Q, Jiang G, Xu C, Zhao C, Xiang Y, Chen Y, Wen S, Zhang H (2014) Ytterbium-doped fiber laser passively mode locked by few-layer molybdenum disulfide (MoS₂) saturable absorber functioned with evanescent field interaction. *Scientific Reports* 4:6346. doi:10.1038/srep06346
19. Roy K, Padmanabhan M, Goswami S, Sai TP, Ramalingam G, Raghavan S, Ghosh A (2013) Graphene-MoS₂ hybrid structures for multifunctional photoresponsive memory devices. *Nat Nanotechnol* 8(11):826–830. doi:10.1038/nnano.2013.206
20. Loan PT, Zhang W, Lin CT, Wei KH, Li LJ, Chen CH (2014) Graphene/MoS₂ heterostructures for ultrasensitive detection of DNA hybridisation. *Adv Mater* 26(28):4838–4844. doi:10.1002/adma.201401084
21. Radisavljevic B, Radenovic A, Brivio J, Giacometti V, Kis A (2011) Single-layer MoS₂ transistors. *Nat Nanotechnol* 6(3):147–150. doi:10.1038/nnano.2010.279
22. Mak KF, Lee C, Hone J, Shan J, Heinz TF (2010) Atomically thin MoS₂: a new direct-gap semiconductor. *Phys Rev Lett* 105(13):136805. doi:10.1103/PhysRevLett.105.136805
23. Giovannetti G, Khomyakov PA, Brocks G, Karpan VM, van den Brink J, Kelly PJ (2008) Doping graphene with metal contacts. *Phys Rev Lett* 101(2):026803. doi:10.1103/PhysRevLett.101.026803
24. Sachs B, Britnell L, Wehling TO, Eckmann A, Jalil R, Belle BD, Lichtenstein AI, Katsnelson MI, Novoselov KS (2013) Doping

- mechanisms in graphene-MoS₂ hybrids. *Appl Phys Lett* 103(25): 251607. doi:10.1063/1.4852615
25. Xu H, He D, Fu M, Wang W, Wu H, Wang Y (2014) Optical identification of MoS₂/graphene heterostructure on SiO₂/Si substrate. *Opt Express* 22(13):15969–15974. doi:10.1364/OE.22.015969
 26. Ju S, Jeong S, Kim Y, Jeon P, Park M-S, Jeong H, Boo S, Jang J-H, Han W-T (2014) Experimental demonstration of surface plasmon resonance enhancement of the tapered optical fiber coated with Au/Ti thin film. *J Non-Cryst Solids* 383:146–152. doi:10.1016/j.jnoncrysol.2013.05.005
 27. Huang Y, Wu D, Chuang C-J, Nie B, Cui H, Yun W (2015) Theoretical analysis of tapered fiber optic surface plasmon resonance sensor for voltage sensitivity. *Opt Fiber Technol* 22:42–45. doi:10.1016/j.yofte.2015.01.004
 28. Yim C, O'Brien M, McEvoy N, Winters S, Mirza I, Lunney JG, Duesberg GS (2014) Investigation of the optical properties of MoS₂ thin films using spectroscopic ellipsometry. *Appl Phys Lett* 104(10):103114. doi:10.1063/1.4868108
 29. Bruna M, Borini S (2009) Optical constants of graphene layers in the visible range. *Appl Phys Lett* 94(3):031901. doi:10.1063/1.3073717
 30. Nair RR, Blake P, Grigorenko AN, Novoselov KS, Booth TJ, Stauber T, Peres NMR, Geim AK (2008) Fine structure constant defines visual transparency of graphene. *Science* 320:1308. doi:10.1126/science.1156965
 31. Maharana PK, Srivastava T, Jha R (2014) On the performance of highly sensitive and accurate graphene-on-aluminum and silicon-based SPR biosensor for visible and near infrared. *Plasmonics* 9(5): 1113–1120. doi:10.1007/s11468-014-9721-4
 32. Maurya JB, Prajapati YK, Singh V, Saini JP, Tripathi R (2016) Improved performance of the surface plasmon resonance biosensor based on graphene or MoS₂ using silicon. *Opt Commun* 359:426–434. doi:10.1016/j.optcom.2015.10.010
 33. Miller MM, Lazarides AA (2006) Sensitivity of metal nanoparticle plasmon resonance band position to the dielectric environment as observed in scattering. *J Opt A Pure Appl Opt* 8(4):S239–S249. doi:10.1088/1464-4258/8/4/s26
 34. Sharma AK, Gupta BD (2005) Fiber optic sensor based on surface plasmon resonance with nanoparticle films. *Photonics and Nanostructures-Fundamentals and Applications* 3(1):30–37. doi:10.1016/j.photonics.2005.06.001